Correlation between density of paramagnetic centers and photovoltaic degradation in polythiophene-fullerene bulk heterojunction solar cells

Reg Bauld,[1] Leesa M. Fleury,[1] Marima Van Walsh,[1] and Giovanni Fanchini[1,2]
[1]*Physics and Astronomy, University of Western Ontario, 1151 Richmond St., London, Ontario N6A 3K7, Canada*
[2]*Chemistry, University of Western Ontario, 1151 Richmond St., London, Ontario N6A 5B7, Canada*

(Received 26 June 2012; accepted 20 August 2012; published online 6 September 2012)

We investigated the physical processes underlying the degradation of poly(3-hexyl-thiophene): phenyl-C_{61}-butyric acid methyl ester (P3HT:PCBM) photovoltaics under harsh environmental conditions during a 70-70-70 test (70% humidity at 70 °C from 0 to 70 h) using a variety of analytical techniques aimed at monitoring moisture incorporation. While the total oxygen content did not significantly increase during the test, a limited fraction of oxygen forms paramagnetic centers in P3HT, PCBM and, more limitedly, P3HT:PCBM heterojunctions. A strong correlation exists between the density of paramagnetic centers and the decay in the AM 1.5 photoconversion efficiency of the devices.
 [http://dx.doi.org/10.1063/1.4749813]

Recent improvements in organic photovoltaics (OPVs) have led to photoconversion efficiencies as high as 8% in these devices,[1,2] making them competitive with amorphous silicon photovoltaics. However, the significant degradation suffered by OPVs, which as of yet is poorly understood, limits their commercialization.

Two main degradation pathways of the active layer have been identified:[3,4] (i) morphological degradation of the bulk heterojunction architecture commonly utilized in OPVs and (ii) chemical degradation of the organic materials, which is predicted to be related to oxygen and moisture incorporation. Poly(3-hexyl-thiophene) (P3HT), a standard donor material in OPVs, has two suggested candidates for chemical degradation: (i) the formation of charge coupled complexes with oxygen[5] and (ii) oxidation of the polymer backbone.[6] Quantification of the oxygen and moisture content in OPVs remains a challenge, with only qualitative results currently available.[7,8] While oxygen and moisture incorporation are universally blamed as the major sources of degradation in OPVs,[6,7,9,10] little information is available on the specific oxygen-related chemical groups that cause decreases in efficiency.

In this letter, we examine the physics behind the degradation of solar cells prepared from P3HT and using phenyl-C_{61}-butyric acid methyl ester (PCBM) as an acceptor material, during a "70-70-70 test" involving the exposure of non-encapsulated P3HT:PCBM active layers to 70% humidity at 70 °C for times up to 70 h. Quantification of oxygen content was performed by Rutherford backscattering (RBS). Specific characterization was done by using electron spin resonance (ESR). ESR on amorphous silicon photovoltaics have demonstrated that a strong relationship exists between the presence of paramagnetic defects and the charge collection efficiency in such material.[11]

The OPV fabrication was carried out as follows: substrates of indium tin oxide-coated glass (90 Ω/□) were treated in a PSD-UV3 Novascan ozone treatment system for 15 min. To prepare the hole blocking layer, poly(3,4-ethylenedioxythiophene):poly(styrenesulfonate) (PEDOT:PSS, Aldrich) was deposited on the substrate by spin coating at 4000 rpm immediately after ozone treatment of the substrate. The resulting film was annealed at 130 °C for 15 min in a VAC Nexus glove box filled with N_2, with oxygen and moisture levels below 5 ppm. To prepare the active layer, 15:15 mg of regioregular P3HT and PCBM (Aldrich) were added to 1 ml chlorobenzene and stirred for 1 h in the glove box. The solution was spin coated at 1500 rpm on top of the PEDOT:PSS film. The sample was then annealed at 130 °C for 15 min. The top contact of the solar cells consisted of thermally evaporated Ca-Al electrodes.

The devices were tested on an AM 1.5 solar simulator (Newport) calibrated using a Sciencetech SC-LT solar cell with certification accredited by the National Institute of Standards and Technology (ISO-17025) and traceable both to the National Renewable Energy Laboratory and the International System of Units. Samples were exposed to the 70-70-70 test in a custom-built chamber with controlled humidity and temperature and were kept in inert atmosphere until they were measured.

RBS spectra were recorded using a 2-MeV $^4He^+$ ion beam at the Tandetron Accelerator at the University of Western Ontario. A region of the solar cell active layer not covered by ITO was used to record the spectra. Our RBS data are reported in Figure 1(a). They show several peaks, with contributions from both the thin films and the substrate. The carbon, oxygen, and sulphur peaks from the film can be identified at energies 500 keV, 720 keV, and 1200 keV, respectively. Preliminary spectra simulations revealed that the contributions to the RBS spectra of the PEDOT:PSS hole-blocking layer (30 nm thickness) are negligible. The O and Si peaks of the substrate (at 600 keV and 1050 keV, respectively) are significant, but due to the energy losses of the $^4He^+$ ions through the organic layers, the peak from oxygen in the films is displaced in energy and can be resolved.

Quantitative data on the film composition were obtained using the SIMNRA simulation package,[12] which takes into account the roughness of the films.[12] These simulations show that throughout the experiment, the oxygen content remains measurably unchanged at ~10 at. % and $(4.5 \pm 1)\cdot 10^{20}$ O atoms/cm^3, as demonstrated in Figure 1(b).

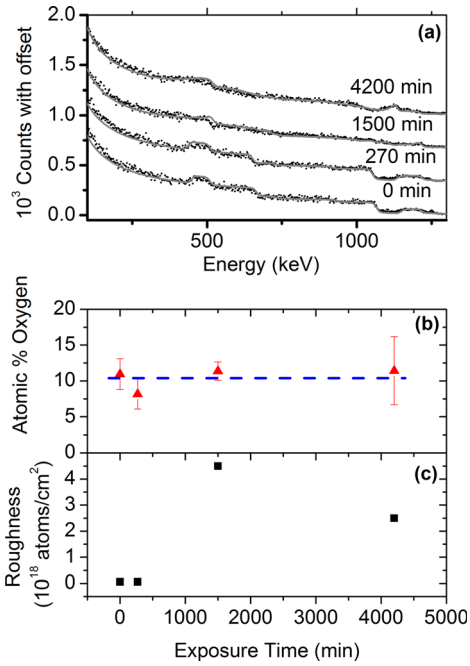

FIG. 1. (a) RBS spectra of P3HT:PCBM solar cells without top electrode, including simulated spectra. (b) Oxygen content vs time as determined by RBS simulations. (c) RBS simulations show increases in roughness under increasing exposure time.

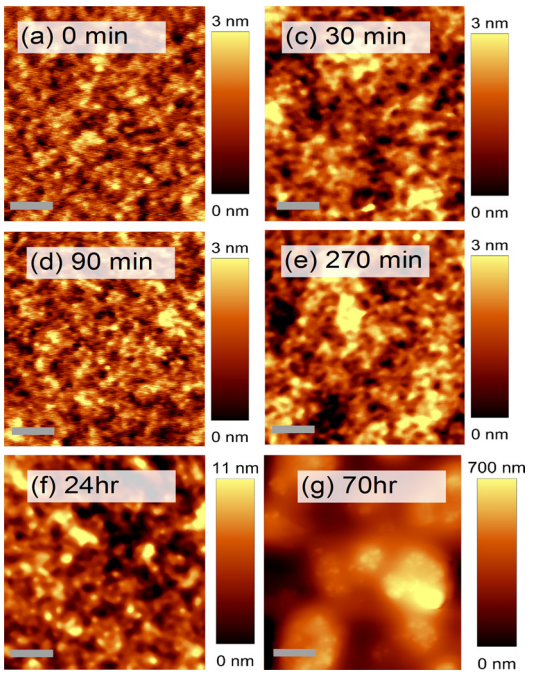

FIG. 2. Atomic force microscopy measurements taken of the P3HT:PCBM active layer under exposure to the 70-70-70 test. The scale bars represent 1 μm. There are significant increases in surface roughness with exposure time that contribute to the incorporation of oxygen into the cell.

Time-of-flight secondary ion mass[13] experiments have also qualitatively shown a negligible increase in oxygen and water content in organic films exposed to isotope enriched water and oxygen environments, which supports our RBS results. This leads us to conclude that any increase in oxygen content is below experimental detection limits. The only evolution clearly visible throughout the spectra is an increasing surface roughness that results in the peak edges becoming broader and shifted in energy. The RBS spectra of the samples at low time of exposure to moisture ($t < 10$ h) are almost identical to each other. Only at $t > 10$ h, did we observe a strong change in roughness that was measurable by RBS. The roughness obtained by RBS simulations is shown in Figure 1(c) and is corroborated by atomic force microscopy (AFM) measurements as discussed below.

Tapping mode AFM images (Witec Alpha300S) were recorded for each complete cell as shown in Figure 2, which shows an ongoing degradation in morphology of the P3HT:PCBM active layer at increasing time of exposure to moisture. From 0 to 10 h, non-uniformity and "grain border corrosion" of the P3HT:PCBM phase proceeds from the boundaries of the nanocrystals. A limited change in nanocrystal size occurs at this stage, even though we can anticipate that a substantial degradation of the AM 1.5 solar cell photoconversion efficiency also occurs (from $\eta = 3.2\%$ down to $\eta = 0.25\%$ after 10 h of treatment). In agreement with RBS measurements, extensive changes in morphology of the solar cell active layers are noticed only at $t > 10$ h of treatment and result in the coalescence of several P3HT and PCBM nanocrystals in larger, smoother, and presumably amorphous domains. This corroborates the increase in overall roughness indicated by RBS, with extensive degradation of the AM 1.5 cell efficiency, which drops to less than $\eta = 0.001\%$ after 70 h of treatment.

ESR measurements were recorded for P3HT, PCBM and P3HT:PCBM bulk heterojunction thin films immediately after removing the samples from the 70-70-xx test. Measurements were taken using a JEOL FA-200 X-band ESR spectrometer equipped with a double-compartment TE_{110} cavity that contained a built-in Mn marker in one of the two compartments for accurate estimates of the spin densities. 100 kHz modulation was applied to detect microwave signal at 0.06 mT amplitude. The ESR measurements were recorded under dark conditions to avoid photo-oxidation of the samples, consistent with the fact that our 70-70-70 test was also performed in the dark.

In Figure 3(a), we observe a rapid increase in spin density of all three sets of samples under short exposure times to moisture. The ESR signal in P3HT has been assigned to many different kinds of paramagnetic defects, including oxygen doping of the polymer chains by the creation of charge coupled complexes,[5,8] oxidization[6] and localized defects introduced by ultraviolet light exposure.[14] A previous study on thick P3HT films suggested that a portion of the signal was due to oxygen doping that increased the number of hole carriers.[8] On the other hand, increase in the spin density was also attributed to an increase in the moisture content of the film, since it was shown[15] that moisture provides a rise in ESR signal similar to that of oxygen.

Our 70-70-70 test confirms that the spin density of our P3HT and P3HT:PCBM thin films must be at least partially assigned to a weak increase of adsorbed water or hydroxyl (OH) groups that are incorporated during our treatment. Fullerenes have also shown similar responses in the presence of oxygen.[5] All of these findings are consistent with our RBS measurements since the measured spin densities ($<10^{18}$ cm^{-3}) indicate that paramagnetic centers are

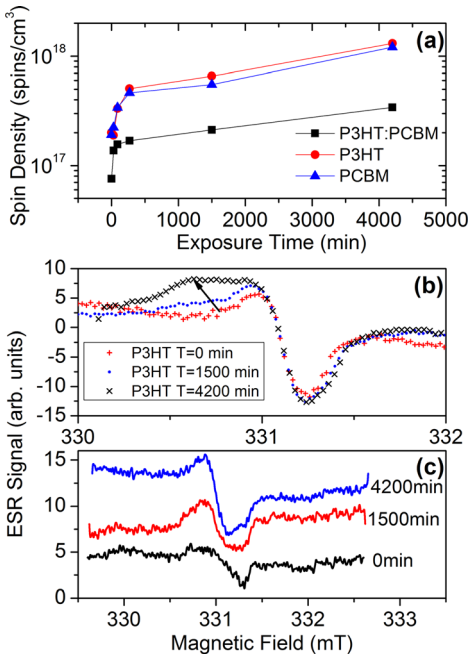

FIG. 3. (a) Spin density vs. time for P3HT, PCBM, and P3HT:PCBM thin films. The drop in spin density in the P3HT:PCBM mix is attributed to the formation of a depletion region between the two phases. (b) ESR spectra of P3HT films. There is a peculiar evolution of the line shape that remains to be explained. (c) ESR spectra of PCBM films at different exposure times show increases in spin density.

incorporated in proportions that are well below the O detection limit of RBS (i.e., ~2 at. % and 10^{20} cm^{-3}).

Surprisingly, we find that, at constant film thicknesses, the spin densities in P3HT:PCBM bulk heterojunctions are consistently lower than in films composed only of P3HT or PCBM, as reported in Figure 3(a). This happens despite the fact that all of our films were prepared, treated, and measured simultaneously. On the other hand, this can be explained by the creation of a depletion region between the two phases. Either hole and electron carriers or moisture-related paramagnetic defects in P3HT and PCBM pair up at the interface between the two phases in a P3HT:PCBM bulk heterojunction. This may decrease the local carrier density and consequentially the total number of unpaired spins, which results in a smaller total spin concentration.

Spectra of selected P3HT and PCBM films are shown in Figures 3(b) and 3(c). At the initial stages of the 70-70-70 test, a broad signal with $g_1 \approx 2.0022$ is observed in both materials, consistent with a signal from delocalized π-electrons as a consequence of oxygen doping.[8] The PCBM films exhibit an increase in intensity as discussed earlier, which is consistent with adsorption of relatively small amounts of oxygen below the RBS detection limit, but the peak shape remains largely unchanged throughout the experiment. The P3HT spectra show the appearance of a second ESR signal at $g_2 = 2.0039$. We propose that this additional ESR feature arises from the progressive incorporation of moisture groups.[16] This is in agreement with the observations of Sperlich *et al.*[6] who hinted that oxidation is responsible for the irreversible degradation of P3HT. Finally, the shape of the ESR signal in P3HT:PCBM bulk heterojunctions can be understood as the superimposition of signals from the individual constituents, P3HT and PCBM.

While Figure 4(b) suggests that the evolution of the spin density N_D as a function of time in our samples follows a multi-stage process ($N_D \sim t^{-1/4}$ for $t \leq 10$ h, corresponding to the "grain border corrosion" phase previously observed by AFM, and $N_D \sim t^{-3}$ for $t \geq 10$ h, corresponding to AFM-detected "extensive degradation" of the samples) the decrease of the AM 1.5 efficiency of our cells at increasing spin density follows a simpler, single-stage exponential decay, as in Figure 4(a). We therefore assign the decline in efficiency of our solar cells to the limited amount of oxygen that is incorporated as moisture-related paramagnetic centers, and not to the overall oxygen or moisture adsorption.

Paramagnetic centers form singly occupied electronic orbitals that act as traps for the recombination of electron-hole pairs.[11] With this in mind, we compared our organic photovoltaics to hydrogenated amorphous silicon (a-Si:H) solar cells, in which an increase in non-radiative recombination is known to be associated with an increase in paramagnetic defect density.[11] In a-Si:H, the collection efficiency as a function of N_D is given by[11]

$$\eta = \frac{\mu_c}{\pi \cdot d^2 \cdot {r_c}^2 v_c N_D}\left[1 - \exp\left(\frac{-\pi \cdot d^2 \cdot {r_c}^2 v_c N_D}{\mu_c V}\right)\right], \quad (1)$$

where V is the applied voltage, d is the film thickness, μ_c is the carrier mobility, and v_c is the thermal velocity of carriers. Equation (1) cannot account for the decrease in efficiency in our cells since it decreases as $\eta \sim {N_D}^{-1}$ for large N_D, while our data in Figure 4(a) can be well fitted to a simple exponential relation

$$\eta = \eta_0 \cdot \exp(-N_D/N_{Cr}), \quad (2)$$

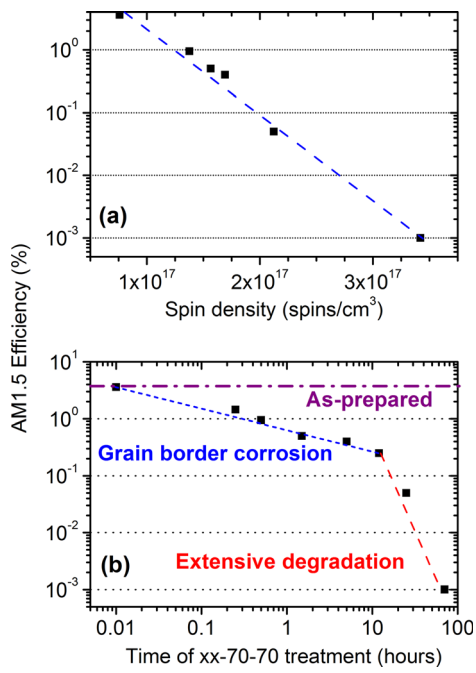

FIG. 4. (a) Spin density measurements of the P3HT:PCBM active layer as a function of solar cell efficiency and exponential relationship with paramagnetic defect density that appears to say the reduction in efficiency depends largely on defect density. (b) Efficiency vs time that shows two stages of degradation, grain border corrosion and extensive degradation

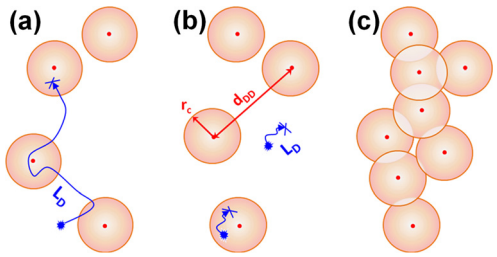

FIG. 5. (a) Exciton diffusion for inorganic materials with $L_D \gg r_c$. (b) Exciton diffusion for organic materials with $L_D \sim r_c$. Excitons created near defects recombine within the vicinity of the defect, while excitons created outside this region are able to separate at a polymer-fullerene interface. (c) At a critical paramagnetic defect density, N_{Cr}, the defects are separated by a distance equal to the Onsager capture radius. This results in percolating regions of defects.

where η_0 is the exponential prefactor and N_{Cr} is the critical spin density for which η decreases by approximately one third. From our best fit, we obtain $N_{Cr} = 3.2 \times 10^{16}\,\mathrm{cm}^{-3}$.

Although full understanding of the simple trend provided by Eq. (2) will require additional theoretical investigations, it is insightful to examine the relationship between the average distance between defects, $d_{DD} \approx \mathrm{N_D}^{-1/3}$, and the Onsager capture radius, defined as the critical distance r_c at which the Culoumbic potential between photoexcited electrons or holes and a charge trapping defect equals the thermal energy $k_B T$

$$r_c = \frac{e^2}{4\pi\varepsilon_r\varepsilon_0 k_B T}, \tag{3}$$

where e is the elementary charge, ε_0 is the vacuum permeability, and ε_r is the dielectric constant of the surrounding material. A value of $\varepsilon_r \approx 3.5$ is common for organic polymers and leads to $r_c \approx 16$ nm[17] at $T = 300$ K. While the difference in r_c between inorganic and organic materials is significant but not dramatic ($\varepsilon_r \approx 13$ gives $r_c \approx 3.5$ nm in a-Si:H[17]), inorganic materials have exciton diffusion lengths of up to 40 μm,[18] which are several orders of magnitude larger than in organic materials where, typically, $L_D \approx 5$–10 nm.[19] Therefore, inorganic solar cell materials are in a regime for which $L_D \gg r_c$, while $L_D \sim r_c$ for organic materials, as shown in Figure 5.

The assumptions used to derive Eq. (1) are no longer valid when $L_D \sim r_c$. In this regime, excitons are highly localized and diffuse poorly throughout the sample. When they are created in the proximity of a trapping defect, their probability to diffuse away and escape non-radiative recombination is minimal because of the short diffusion length that prevents virtually any excitons created at $r < r_c$ from a defect to dissociate and contribute to the photocurrent. Conversely, excitons photogenerated at $r > r_c$ have the ability to be dissociated at a polymer-fullerene interface without being captured.

The volume fraction of material for which the condition $r > r_c$ holds is determined by the average distance between defects and, consequently, the defect density. When $N_D < N_{Cr}$, defects are extremely sparse and only a minimal fraction of excitons are generated within the capture radius of a defect. At the opposite, the probability of capture and nonradiative recombination of an exciton at a charge trapping defect increases dramatically for $N_D > N_{Cr}$, when the volume fraction of material for which $r < r_c$ forms a system of percolating spheres. It is interesting to note that the percolation threshold, at which $d_{\mathrm{DD}} \approx 2r_c$, is reached exactly at $N_D = N_{Cr}$, where $d_{DD} \approx N_{Cr}{}^{-1/3} \approx 32$ nm.

In summary, we have shown that at the critical defect density N_{Cr} for which P3HT:PCBM solar cells undergo the most significant degradation, the Onsager capture radius equals the average distance between paramagnetic defects. This observation corroborates an inverse-exponential correlation between paramagnetic defect density and cell efficiency, which we find to hold irrespectively of both the complex changes in morphologies undergone by the cells during our 70-70-70 test and the fact that the total O content (measured using RBS) does not significantly change during our experiments. Our results strongly support the hypothesis that oxygen degrades organic solar cells only when incorporated in the form of paramagnetic defects. These findings may have important applications for designing encapsulation systems for organic solar cells of improved performance.

We would like to thank Professor Peter Simpson for valuable discussions about the RBS measurements. L.M.F. acknowledges an NSERC-USRA award. G.F. acknowledges funding in the form of a Canada Research Chair (CRC) and an Early Researcher Award (ERA) from the Ontario Ministry of Research and Innovation. This work was partially supported by an NSERC-Discovery Grant.

[1]H. Y. Chen, J. H. Hou, S. Q. Zhang, Y. Y. Liang, G. W. Yang, Y. Yang, L. P. Yu, Y. Wu, and G. Li, Nat. Photonics **3**(11), 649–653 (2009).
[2]M. A. Green, K. Emery, Y. Hishikawa, and W. Warta, Prog. Photovoltaics **18**(5), 346–352 (2010).
[3]J. A. Hauch, P. Schilinsky, S. A. Choulis, R. Childers, M. Biele, and C. J. Brabec, Sol. Energy Mater. Sol. Cells **92**(7), 727–731 (2008).
[4]M. Jorgensen, K. Norrman, and F. C. Krebs, Sol. Energy Mater Sol. Cells **92**(7), 686–714 (2008).
[5]M. D. Pace, T. C. Christidis, J. J. Yin, and J. Milliken, J. Phys. Chem. **96**(17), 6855–6858 (1992).
[6]A. Sperlich, H. Kraus, C. Deibel, H. Blok, J. Schmidt, and V. Dyakonov, J Phys. Chem. B **115**(46), 13513–13518 (2011).
[7]K. Norrman, S. A. Gevorgyan, and F. C. Krebs, ACS Appl. Mater. Interfaces **1**(1), 102–112 (2009).
[8]M. S. A. Abdou, F. P. Orfino, Y. Son, and S. Holdcroft, J. Am. Chem. Soc. **119**(19), 4518–4524 (1997).
[9]A. Seemann, H. J. Egelhaaf, C. J. Brabec, and J. A. Hauch, Org. Electron. **10**(8), 1424–1428 (2009).
[10]J. Schafferhans, A. Baumann, A. Wagenpfahl, C. Deibel, and V. Dyakonov, Org. Electron. **11**(10), 1693–1700 (2010).
[11]R. A. Street, *Hydrogenated Amorphous Silicon* (Cambridge University Press, 2005).
[12]M. Mayer, AIP Conf. Proc. **475**(1), 541–544 (1999).
[13]K. Norrman, M. V. Madsen, S. A. Gevorgyan, and F. C. Krebs, J. Am. Chem. Soc. **132**(47), 16883–16892 (2010).
[14]A. Konkin, H. K. Roth, P. Scharff, A. Aganov, O. Ambacher, and S. Sensfuss, Solid State Commun. **149**(21–22), 893–897 (2009).
[15]S. Hoshino, J. Appl. Phys. **95**(9), 5088 (2004).
[16]W. L. Ma, C. Y. Yang, X. Gong, K. Lee, and A. J. Heeger, Adv. Funct. Mater. **15**(10), 1617–1622 (2005).
[17]T. M. Clarke and J. R. Durrant, Chem. Rev. **110**(11), 6736–6767 (2010).
[18]J. D. Cuthbert, Phys. Rev. B **1**(4), 1552–1557 (1970).
[19]P. E. Shaw, A. Ruseckas, and I. D. W. Samuel, Adv. Mater. **20**(18), 3516–3520 (2008).